Precision Clinical Medicine, 4(3), 2021, 192–203

https://doi.org/10.1093/pcmedi/pbab018
Advance Access Publication Date: 26 July 2021
Review

REVIEW

Understanding the predictive value and methods of risk assessment based on coronary computed tomographic angiography in populations with coronary artery disease: a review

Yiming Li[§], Kaiyu Jia[§], Yuheng Jia, Yong Yang, Yijun Yao, Mao Chen* and Yong Peng*

Department of Cardiology, West China Hospital, Sichuan University, Chengdu 610041, China

*Correspondence: Yong Peng, pengyongcd@126.com; Mao Chen, hmaochen@vip.sina.com
Kaiyu Jia, http://orcid.org/https://orcid.org/0000-0002-8954-2636
[§]Yiming Li and Kaiyu Jia contributed equally to this work.

Abstract

Risk assessment in coronary artery disease plays an essential role in the early identification of high-risk patients. However, conventional invasive imaging procedures all require long intraprocedural times and high costs. The rapid development of coronary computed tomographic angiography (CCTA) and related image processing technology has facilitated the formulation of noninvasive approaches to perform comprehensive evaluations. Evidence has shown that CCTA has outstanding performance in identifying the degree of stenosis, plaque features, and functional reserve. Moreover, advancements in radiomics and machine learning allow more comprehensive interpretations of CCTA images. This paper reviews conventional as well as novel diagnostic and risk assessment tools based on CCTA.

Key words: coronary computed tomographic angiography (CCTA); coronary artery disease; risk assessment; prediction value

Background

Ischaemic heart disease (IHD) has become a global healthcare concern in recent years.[1] Among IHDs, coronary artery disease (CAD) is one of the leading causes of myocardial ischaemia.[2] Risk assessments in the CAD population play a pivotal role in the early identification of high-risk patients as well as the optimization of treatment options such as medication, coronary intervention, or surgery, thus improving prognosis.[3] The conventional evaluation of CAD relies heavily on invasive imaging procedures. To date, invasive coronary angiography (ICA) has been the most widely adopted technique due to its performance in quantifying the degree of stenosis of coronary arteries.[4] Both intravascular ultrasound (IVUS) and optical coherence tomography (OCT) have also been used in addition to ICA to obtain a more comprehensive view of atherosclerotic lesions.[5–7] However, all these techniques are invasive approaches

Received: 30 May 2021; **Revised:** 23 July 2021; **Accepted:** 23 July 2021

with relatively long intraprocedural times and high costs.

Later, in 1998, spiral multidetector CT further improved the spatial and imaging quality of computed tomorgraphy (CT), fuelling the rapid development of CT technology in the clinical management of cardiovascular disease. Furthermore, coronary computed tomographic angiography (CCTA) allows physicians to obtain high-quality images of coronary anatomy in a shorter period of time, enhancing the diagnostic accuracy. Compared with ICA, CCTA has a higher specificity (90%–95%), which makes it an effective tool for excluding CAD as a diagnosis.[8,9] Thus, CCTA has become the first-line diagnostic tool in the clinical management of CAD. According to current guidelines, CCTA is the recommended tool for screening (Class I, Level B) and risk stratification (Class I, Level B) in CAD.[3] Multiple novel evaluation and diagnostic tools have been derived from CCTA and CCTA-based imaging techniques. These tools can provide further information beyond the basic cardiovascular anatomy and morphology characteristics. Thus, we performed a literature search on EMBASE, Ovid, and PubMed with the following search terms: coronary computed tomographic angiography; risk assessment; prognostic value; prediction model; high risk signs; fractional flow reserve; radiomics; machine learning; deep neural networks. This study aimed to conduct a comprehensive review regarding conventional as well as novel diagnostic and risk assessment tools based on CCTA.

Risk assessment based on anatomical characteristics of the coronary artery

CCTA is being applied in a widening range of clinical scenarios due to its ability to locate the affected coronary segment with precision and speed.[10,11] Previous studies have shown that this modality has a sensitivity of 75%–90% and a specificity of 90%–95% in terms of diagnosing haemodynamic abnormalities caused by coronary stenosis.[8] According to a meta-analysis that included 27 studies, 64-slice CCTA has a sensitivity of 87% (95% CI: 86.5%–88%), a specificity of 96% (95% CI: 95.5%–96.5%), and a total accuracy of 94% in terms of detecting coronary stenosis relative to traditional invasive approaches such as ICA.[8] The high negative predictive value (>95%) makes CCTA an efficient tool for excluding CAD as a diagnosis, which has proven to be of great value in the clinical management of acute chest pain.[12] Compared with other noninvasive approaches, such as cardiac magnetic resonance imaging, single-photon emission computed tomography, or stress echocardiography, CCTA has the highest accuracy in diagnosing CAD patients presenting with acute chest pain. Patients with normal CCTA results have a relatively low incidence of adverse cardiovascular events within a year of discharge (<1%). Moreover, the implementation of emergency CCTA in patients with acute chest pain reduces medical expenses and shortens hospital stays.[13]

Several studies have focused on the predictive value of CCTA in evaluating coronary stenosis. Hadamitzky et al. found that the use of CCTA to classify CAD patients into those with or without obstructive arteries exhibited a greater long-term predictive value than the Framingham risk score.[14] Min et al. also observed the predictive values of CCTA findings (including the degree, location, quantity and properties of coronary stenosis) for long-term prognosis and established three risk algorithms: segment stenosis score (SSS), segment involvement score, and 3-vessel plaque score.[15] All three risk scores have high discriminatory power in predicting the long-term cumulative survival rate. In the CONFIRM study, patients were categorized as non-CAD, nonobstructive CAD (a ≤50% luminal diameter stenosis in a major coronary artery), nonhigh-risk obstructive CAD (a ≥50% luminal diameter stenosis in a major coronary artery), and high-risk obstructive CAD (patients with at least two-vessel obstructive CAD with proximal left anterior descending artery involvement, three-vessel CAD, or left main CAD).[16] After a median follow-up of 22 months, the all-cause mortality rates were 0.65%, 1.99%, 2.90%, and 4.95%, respectively, with significant differences in survival between groups ($P < 0.001$). Multivariate Cox regression analysis was conducted with the mentioned subgroups as categorical variables, and the hazard ratio (HR) was 1.58 (95% CI: 1.42–1.76). When combined with clinical characteristics such as age, sex, symptoms, and National Cholesterol Education Program Expert Panel on Detection, Evaluation, and Treatment of High Blood Cholesterol in Adults (Adult Treatment Panel III) (NCEP ATP III) score, the receiver operating characteristics (ROC) curve analysis for long-term mortality demonstrated an area under the curve (AUC) of 0.75, which was better than that of left ventricular ejection fraction-based risk models (AUC = 0.68, $P < 0.001$). Additionally, high-risk obstructive CAD patients benefited more from surgical interventions than from medication (HR = 0.22; 95% CI 0.11–0.47), indicating the potential use of CCTA in CAD patients receiving cardiac surgery or interventions.[17] Subsequent studies created an online risk scoring system and included factors such as affected proximal segment (≥50% luminal diameter stenosis), mixed or calcified plaques in proximal segments and NCEP ATP III score.[18] The machine learning-based CONFIRM score has been suggested to have better predictive value than conventional risk scores in both the training and test sets.

The CAD-RADS scoring system published in 2016 ranked CAD stenosis severity as 0 (0%), 1 (1%–24%), 2 (25%–49%), 3 (50%–69%), 4A (70%–99% in 1–2 vessels), 4B (70%–99% in 3 vessels or ≥ 50% left main), or 5 (100%).[19] The study also provided further descriptions and performed evaluations on patients with different risk levels. CAD-RADS is an efficient scoring system with outstanding discriminatory power. The cumulative 5-year survival

ranged from 95.2% in patients considered level 0 to 69.3% in patients considered level 5. The ROC curve for predicting all-cause mortality or myocardial infarction (MI) was 0.7052 for CAD-RADS, which was noninferior to that of the Duke Index (AUC = 0.7073).[20]

The accuracy of CCTA in evaluating coronary stenosis serves as the cornerstone of its rapid development and wide dissemination. As previously mentioned, multiple large-scale clinical trials have shown the efficacy of CCTA in the risk stratification of CAD patients. Although there are several theories for interpreting the results of CCTA, its widespread application in clinical settings requires easily obtained risk scores. The currently available scoring systems are outlined in Table 1.

Identifying high-risk patients based on morphological characteristics in CCTA findings

Histological studies have shown that coronary plaques play a vital role in the progression of endothelial damage and atherosclerosis.[21,22] The morphology, composition and inflammatory process of atheroma plaques have more clinical implications for the identification of high-risk CAD patients than the degree of stenosis alone.[23] Acute coronary syndrome (ACS) is a disease with rapid progression and poor prognosis. Various underlying mechanisms of ACS have been proposed, including plaque rupture, plaque erosion, calcifications, and spasms of the epicardium vessels or arterioles.[24,25] Studies based on biopsies have indicated that plaque rupture is the leading cause of fatal coronary embolism (>70%).[26,27] These ruptured plaques are termed vulnerable plaques or high-risk plaques (HRPs). Davies et al. summarized the features of these plaques as follows: a large lipid core with macrophage infiltration, a thin fibrous cap (<65 μm), positive remodelling (PR) or spotty calcifications (SC).[28,29] The early identification of HRPs in high-risk patients based on these features is crucial to improving prognosis. Invasive tests are the gold standard in diagnosing atheroma plaques. Compared with IVUS, OCT provides a better resolution (10 μm) but a lower depth of penetration. Although both methods can be used to evaluate plaque formation in CAD, neither is widely adopted due to their high costs and invasiveness.

As a promising diagnostic tool, CCTA not only is able to measure the degree of coronary stenosis, but also can visualize the morphology and composition of plaques. Plaques with thin fibrous caps (<65 μm) cannot be detected by CCTA due to its limited resolution. However, certain plaque features observed by CCTA have a proven correlation with the occurrence of major adverse cardiac events (MACEs) and overall prognosis, so this method may be useful in risk stratification.[30,31] Low attenuation plaque (LAP), also known as soft plaque, has a CT value less than 30–60 HU and can be viewed as an HRP with a large lipid core.[27,32] PR is indicated by a remodelling index (RI) greater than 1.1, which is defined as the ratio between the diameter of the largest remodelled vessel and the reference vessel.[33] SCs are calcified plaques that are less than 3 mm in all dimensions.[34] The Napkin ring sign (NRS) is characterized by a plaque core with low CT attenuation surrounded by a rim-like area of higher CT attenuation.[35] A meta-analysis including 18 studies revealed that according to CCTA, compared with stable angina, ACS has a higher rate of SCs (odds ratios (OR): 1.42, 95% CI (1.05–1.92), $P = 0.023$), a higher percentage of LAP with CT value < 30 HU (OR: 4.1, 95% CI (2.5–5.7), $P < 0.0001$), and higher RI (weighted mean difference (WMD), 95% CI (0.25–0.70)).[36] Additionally, compared with patients with low-risk plaque, HRP patients had a higher incidence of ACS during follow-up (26% vs. 22%, OR: 12.14, 95% CI (5.2–28.1), $P = 0.0001$).[36] Another meta-analysis[37] suggested that HRP is strongly correlated with the occurrence of MACEs based on long-term follow-up. The HRs for LAP, NRS, SC, and PR were 2.95 (95% CI, 2.03–4.29), 5.06 (95% CI, 3.23–7.94), 2.25 (95% CI, 1.26–4.04), and 2.58 (95% CI, 1.84–3.61), respectively.

Despite the correlation between HRP and coronary events, risk models based on these characteristics remain lacking. In the ROMICAT II study, risk models based on the characteristics of HRPs had a superior predictive value for ACS events than conventional risk models, which were based only on the degree of stenosis (AUC = 0.91 vs. 0.85, $P = 0.002$).[38] In a large-scale cohort study published in 2019,[39] the cumulative 5-year all-cause mortality rate was significantly higher in CAD patients with HRP than in those without HRP (21.7% vs. 5.1%, $P < 0.001$). The same conclusion was drawn with other cardiovascular endpoints. No significant differences were found between CAD patients with no HRP and non-CAD patients, indicating that HRP is a reliable marker in the progression of CAD. Other than the aforementioned features of HRP, a recent study has proven that the perivascular fat accumulation is strongly associated with coronary inflammation.[40] In the Cardiovascular RISk Prediction using Computed Tomography (CRISP-CT) study, a novel imaging biomarker called the perivascular fat attenuation index (FAI) demonstrated promising predictive value (HR: 2.06, 95% CI (1.50–2.83), $P < 0.0001$). Thus, perivascular imaging in CCTA may also be of great value in the risk assessment of CAD patients.[41]

The physiological functions of the coronary artery based on CT

Neither the degree of stenosis nor plaque characteristics are a direct reflection of the extent of myocardial ischaemia. Based on ICA, fractional flow reserve (FFR) is able to detect the reversible ischaemia of the myocardium that could lead to disease progression.[42] Regarding its use in revascularization procedures such as percutaneous coronary intervention or coronary artery

Table 1. The risk assessment tools derived from coronary computed tomographic angiography.

Names of tools	Authors or collaboration	Year	Features to develop models	Estimate methods	Model evaluation
Segment stenosis score Segment-involvement score 3-vessel plaque score Modified Duke index	James K. Min	2007	The stenosis severity, location and numbers of lesions in coronary tree	Multivariable Cox proportional hazards models	Survival analysis for all-cause mortality during follow up All the tools showed ability to partition cumulative death.
CONFIRM Score	CONFIRM registry	2013	NCEP ATP III score, the number of proximal segments with stenosis >50%, and the number of proximal segments plaques (mixed or calcified)	Multivariable Cox proportional hazards models	Highest AUC in both test and validation sample for all-cause mortality, compare to Morise, Framingham, and NCEP ATP III score
CAD-RADS	SCCT, ACR, and NASCI	2016	Degree of maximal coronary stenosis (including left main and 3-vessel disease)	Multivariable Cox proportional hazards models	The ROC curve for prediction of death or MI was 0.7052 for CAD-RADS, was comparable with the Duke Index and traditional CAD classification.
ROMICAT score	ROMICAT II trail	2015	High-risk plaque feature, including positive remodelling, low CT attenuation plaque, spotty calcium or plaque length	Multivariable logistic regression analyses	ROMICAT score could improve model contained stenosis and gender for prediction of ACS.
NA	CRISP-CT study	2018	Perivascular FAI: defined as fat within a radial distance equal to the diameter of three major coronary artery.	Multivariable Cox regression	Perivascular FAI enhances the prediction and restratification in cardiac risk over current assessment tool in CCTA.
NA	EMERALD study	2018	CT-FFR, diameter stenosis, wall shear stress and high-risk plaque feature	Marginal Cox regression analysis	CT-FFR and other haemodynamic parameters could improve the discrimination and accuracy of models in prediction of ACS.
NA	Márton Kolossváry	2019	Radiomic parameters from CCTA	Eight machine learning models	Radiomics features with machine learning analysis outperformed visual assessment in the identification of high-risk plaque.
NA	CONFIRM registry	2016	The features with information gain > 0, including 35 CCTA parameters and 19 clinical features	Machine learning (LogitBoost)	The LogitBoost model had a significantly higher AUC for all-cause mortality prediction than all other scores, which were Framingham score, SSS, SIS, and modified Duke index.
ML-IRS	NXT trial	2021	Quantitative CCTA measures with information gain > 0 plus age and gender	Ensemble classification boost	ML-IRS improved the prediction of revascularization in patients with coronary artery disease.

ACS: acute coronary syndrome; ACR: the American College of Radiology; AUC: area under the curve; CAD: coronary artery disease; CCTA: coronary computed tomographic angiography; CT: computed tomography; FAI: perivascular fat attenuation index; FFR: fractional flow reserve; MI: myocardial infarction; ML-IRS: machine learning ischaemia risk score; NA: not available; NASCI: North American Society for Cardiovascular Imaging; NCEP ATP III: National Cholesterol Education Program Expert Panel on Detection, Evaluation, and Treatment of High Blood Cholesterol in Adults (Adult Treatment Panel III); ROC: receiver operating characteristic; SCCT: Society of Cardiovascular Computed Tomography; SIS: segment-involvement score; SSS: segment stenosis score.

bypass graft, FFR has achieved better prognostic predictions than ICA.[43–45] Current guidelines recommend that when noninvasive coronary evaluations are not possible, FFR should be used in the assessment of the coronary artery in revascularization procedures (Level I, Class A).[46]

CT-FFR is a noninvasive approach that demonstrates coronary perfusion based on the processing of CCTA images. A high-speed computer enables the processing of images through computational fluid dynamics (CFD) and machine learning, constituting the very foundation of CT-FFR. The results of CT-FFR are obtained through the following steps: (1) reconstruct the 3D anatomy of the coronary artery tree based on CCTA; (2) calculate baseline coronary perfusion based on the volume of the coronary artery tree; (3) establish the hyperaemia model according to the impact of adenosine on microcirculation resistance; and (4) calculate coronary perfusion pressure using the Navier–Stokes equation and create a colour-coded 3D-FFR anatomy model.[47] Currently, there are three types of CT-FFR systems: the FDA-approved FFR_{CT} (HeartFlow Inc., Redwood City, CA)[48]; the CFDA-approved DEEPVESSEL FFR (Shenzhen Keya Medical Technology Co., Ltd, Shenzhen, China); and the cFFR by Siemens (Siemens Medical Solutions; Forchheim, Germany), which is a relatively simplified device that is awaiting approval.

CT-FFR is a promising diagnostic tool for the evaluation of physiological coronary function based on image processing from CCTA. This method reduces radiation exposure and avoids unnecessary medications. To date, FFR_{CT} is the most frequently used system. According to three randomized controlled trials, FFR_{CT} has a high accuracy with an invasive FFR $\leq$ 0.8 as the diagnostic criterion.[49–51] The sensitivity, specificity, positive predictive value, and negative predictive value of the three versions of FFR_{CT} (1.0–1.2–1.4) ranged from 84% to 89%, 61% to 86%, 56% to 74%, and 84% to 95%, respectively. The AUC ranged from 0.79 to 0.93. Multiple single-centre cohort studies on cFFR also suggested similar results.[52–54] A prospective cohort study with 68 individuals who adopted the DEEPVESSEL FFR system found that compared with invasive FFR, this system had a sensitivity of 97%, specificity of 75%, positive predictive value of 82%, negative predictive value of 95%, and an AUC of 0.93.[55] Thus, CT-FFR has a high diagnostic accuracy and has improved the specificity of the evaluation of coronary stenosis compared with that of CCTA alone. CT-FFR aids the risk stratification of CAD patients with CCTA images, avoiding unnecessary invasive procedures.

Currently, it is recommended that patients with a medium to high degree of coronary stenosis (30%–90% luminal diameter stenosis, as indicated by CCTA) undergo further CT-FFR.[56] However, the concomitant calcification in patients with severe stenosis or complete occlusion of coronary vessels may limit the use of CT-FFR. Previous studies have arrived at a consensus that the use of CT-FFR is of maximal benefit in the risk assessment and treatment of patients with moderate stenosis. Compared with analysis based solely on CCTA, CT-FFR greatly improved the specificity in detecting ischaemic lesions and thus subsequently contributed to the cost-effectiveness in CAD management.[52] An FFR value of 0.8 is the cut-off for medication therapy or revascularization procedures.[56] The PLATFORM study showed that FFR_{CT} significantly decreased the percentage of nonobstructive CAD patients receiving cardiac interventions (73.3% vs. 12.4%, $P < 0.001$).[57] From a socioeconomic standpoint, FFR is also associated with reduced medical expenses, even after taking into account the costs of the FFR exam itself ($9036 vs. $12 145, $P < 0.0001$). In the largest real-world study to date (Assessing Diagnostic Value of Noninvasive FFR-CT in Coronary Care, ADVANCE), 72.3% of the patients with an FFR_{CT} value $\leq$ 0.8 underwent invasive treatments after reevaluation.[58] Both the MACE rate and the MI/all-cause mortality rate within 90 days of follow-up for patients with an FFR_{CT} value >0.8 were 0%. In contrast, the all-cause mortality rate and MACE rate for patients with an FFR_{CT} value $\leq$0.8 were 0.6% ($P = 0.0019$) and 0.45% ($P = 0.0070$), respectively. The results reflect the high discriminatory power of FFR. In addition, according to the EMERALD study by Lee et al.[59,60] the culprit vessels in ACS patients showed lower CT-FFR values than the nonculprit vessels (0.72 ± 0.17 vs. 0.79 ± 0.14, $P = 0.006$), and greater differences were observed in the CT-FFR values before and after the culprit lesion was excised (0.17 ± 0.17 vs. 0.06 ± 0.07, $P < 0.001$). The risk model combining the degree of stenosis, high-risk haemodynamic parameters (CT-FFR $\leq$ 0.8 or ΔCT-FFR $\geq$ 0.06) and HRP characteristics obtained by CT-FFR exhibited the best predictive value for ACS. The concordance statistic (c-index) was 0.789, which was higher than that for the risk model based only on HRP characteristics and the degree of stenosis (c-index = 0.747, $P = 0.014$). In the marginal Cox hazard ratio model, with HRP (–) and high-risk haemodynamics (–) as baseline hazard functions, the HR for patients with both HRP (–) and high-risk haemodynamics was 11.753. The results show promising potential techniques that can yield data on both coronary physiological function and plaque morphology in CAD risk stratification.

Quantitative analysis to obtain plaque parameters by radiomics

Radiomics was first introduced by the Dutch radiation oncologist Lambin in 2012; it aims to extract quantitative features from radiographic images and create a data set accordingly.[61] These features contain thousands of parameters, and radiomics establishes a correlation among these parameters themselves as well as between these parameters and clinical data. New markers and risk models derived from these results improve the diagnostic accuracy of radiographic imaging and expand our perception of the pathophysiological process of certain diseases.

As previously stated, different stages of coronary atherosclerosis manifest differently on CT imaging. Qualitative features, such as those of HRP, have already been proven to be closely correlated with MACEs.[62] Instead of qualitatively analysing features, radiomics quantifies the results by calculating various parameters, thus improving the accuracy and objectivity. There are four steps involved in radiomics analysis:[63] (1) Intensity-based extraction, also known as first-order statistics, involves the simple statistical analysis of pixels or voxels, such as the calculation of the mean or standard deviation. Although radiomics is a relatively new concept, it has already been applied in the coronary artery calcium score and other diagnostic tools. (2) Texture-based extraction,[64] including the grey-level cooccurrence matrix[65] and grey-level run-length matrix (GLRLM),[66] turns voxels into matrices through mathematical analysis. (3) Shape-based extraction, including 1D, 2D, and 3D measurements and Minkowski Functionals,[67] demonstrates the spatial distribution of plaques. (4) Transform-based extraction uses methods such as Fourier transforms[68] to transform the images from the spatial domain to the frequency domain, making the features more suitable for calculations.

Although the calculations and models used in radiomics are not novel, their application has remained superficial for many years. Due to machine learning and computer-based quantitative image processing technology, radiomics is being applied in clinical settings at an accelerated pace. In the field of cardiology, the radiology team led by Márton Kolossváry and Pál Maurovich-Horvat conducted a systematic analysis and explorative validation regarding CCTA-based radiomics.[63] In a clinical trial of 60 patients,[69] researchers used the R programming language and their own radiomics image analysis to extract 4440 radiomics features. After selection, 916 (20.6%) features were proven to be associated with NRS. For the prediction of NRS, half of the features (440/916) had an AUC $>$ 0.80. The parameters obtained by GLRLM had the best predictive value and an AUC of 0.918. These parameters greatly exceeded those of traditional CCTA-based methods, such as attenuation characteristics and plaque volume (AUC: 0.508–0.770). In subsequent studies, radiomic parameters significantly outperformed measurements of noncalcified plaque volume to identify attenuated plaque by IVUS (AUC: 0.72 vs. 0.59, $P < 0.001$); radiomics also outperformed traditional LAP features (i.e. the presence of low attenuation voxels) to identify thin-cap fibroatheroma by OCT (AUC: 0.80 vs. 0.66, $P < 0.001$). Finally, radiomics outperformed high-risk features in identifying NaF^{18} positivity (AUC: 0.87 vs. 0.65, $P < 0.001$).[70] Radiomics demonstrated a good diagnostic accuracy in terms of identifying invasive and radionuclide imaging markers of HRPs and evaluating plaque vulnerability. Radiomics features also exhibited significant advantages compared with other conventional high-risk features. In addition to CAD, radiomics parameters also showed promising results in recognizing pannus formation in prosthetic valve obstruction after valve replacement surgeries (AUC = 0.876).[71] As we are embracing the rapid development of transcatheter aortic valve implantation technology, radiomics may be used to evaluate valve failure after bioprosthesis replacement procedures and guide cardiac care teams in developing treatment protocols.

It is worth mentioning that radiomics and machine learning can be combined almost seamlessly due to their endogenous theoretical features. The high-dimensional data set recognized by radiomics can be reduced into low-dimensional data by machine learning. Because these data are derived from the transformation and normalization of images, the high-order fitting of machine learning has greater proficiency than that of conventional statistical analysis. Kolossváry et al. found that radiomics models built on machine learning were able to improve the recognition of high-risk coronary abnormalities (AUC = 0.73).[70] However, the flaws of radiomics and machine learning are very similar as well. Although radiomics provides a more subjective quantitative analysis of images and has higher accuracy in HRP recognition, radiomics markers and models lack a theoretical foundation. This problem is similar to the problem of machine learning interpretability: specifically, the more complex and higher dimension the mathematical tools are, the more difficult it is to interpret the results. This is an obstacle that needs to be addressed in the quantitative evaluation of patients by CCTA, precision-individual medicine, and artificial intelligence in medicine.

Machine learning, CAD, and coronary CT

Machine learning can be viewed as a branch of artificial intelligence (AI). Based on mathematics and computer science, machine learning involves the study of large amounts of data and subsequent classification or prediction of new data. The theories of machine learning, such as regularization, clustering, cross-validation, and use of numerous algorithms, have been widely applied to clinical research and big data analytics. Classic algorithms, including logistic regression, the Gaussian Bayes classifier, decision trees, and random forest and gradient ascending algorithms such as XGBoost, have already demonstrated excellent proficiency in analysing structuralized medical data with better predictive value than conventional risk assessment tools based on statistical analysis.[72,73] Deep learning, an algorithm built on artificial neural networks (ANNs), outperforms medical professionals in terms of analysing consecutive information (medical images or sensors) and complex correlations in genomic data.[74,75] Deep learning has already become a powerful tool in the field of oncology and psychiatric disorders.[76,77] Both CCTA images and the information obtained by CCTA images can feasibly be analysed by machine learning to conduct risk assessments due to their detailed features and unproven correlations.

Risk assessment based on conventional machine learning algorithms

The detection of calcified plaques by CCTA can reduce medical expenses due to unnecessary noncontrast CT imaging and avoid radiation exposure. Machine learning offers a new approach to improve CCTA technology. Mittal et al. suggested that probabilistic boosting-tree and random forest were able to accurately detect calcified plaques in CCTA, and random forest demonstrated a detection rate of 90%.[78] According to Yang et al., a support vector machine (SVM) enhanced the detection of coronary calcifications in CCTA.[79] Focusing on plaque features, the NXT randomized controlled trial analysed the high-risk factors for patients and HRPs detected by CCTA using information gain and revealed that the difference in contrast concentration, plaques with low attenuation and noncalcification, noncalcified plaque, and plaque volume were the most important features in predicting stenosis with an FFR < 0.8. The risk model of these features (built by LogitBoost) had an AUC of 0.84 in predicting stenosis with an FFR < 0.8, which was better than that of the risk models built on the degree of coronary stenosis (AUC $= 0.76$, $P = 0.005$) and CAD pretest probability (AUC $= 0.63$, $P < 0.0001$).[80] Another study also found that risk models of plaque features built based on SVMs outperformed radiologists in predicting stenotic CAD (AUC $= 0.94$).[81] Damini Dey et al. built the machine learning ischaemia risk score (ML-IRS) based on various CCTA imaging features. ML-IRS was superior than conventional risk assessment tools in terms of predicting revascularization (AUC $= 0.69$ to 0.78, $P < 0.0001$).[82]

The CONFIRM study is a good example of how to predict long-term prognosis based on CCTA information using machine learning. In a study published in 2016,[83] 10 030 suspected CAD patients were included, and the mean follow-up duration was 5.4 ± 1.4 years. The data set contained 20 clinical features and 40 CCTA parameters. Parameters with information gain > 0 (19 clinical features and 35 CCTA parameters) were included in the risk model. A subsequent risk model for predicting the 5-year all-cause mortality rate was built using LogitBoost, and 10-fold cross-validation was conducted. The risk model was proven to be better than conventional clinical risk assessments and had an AUC of 0.79. The risk model classifies patients into low-risk, intermediate-risk, and high-risk groups. The mortality rates of the three subgroups were 1.8%, 6.7%, and 27%, respectively. The validation curve demonstrated high uniformity with the actual mortality rate and had a Brief score of 0.08. Thus, machine learning has excellent discrimination and calibration abilities in predicting clinical outcomes. Another study published in 2018 by the CONFIRM investigators demonstrated a similar proficiency in predicting the composite endpoint of all-cause mortality and MI using a risk model based on 35 CCTA parameters built by XGBoost. The AUC was 0.771, which was better than that of the SSS (AUC $= 0.701$, $P < 0.001$).[84]

Deep learning and neural networks for CCTA images

One of the major uses of deep learning in the analysis of CCTA images is the calculation of CT-FFR. Unlike FFR_{CFD}, machine learning/deep learning inputs features, then conducts fitting through ANN, and eventually outputs FFR_{ML}. Itu et al. first introduced this method and calculated the value of CT-FFR with an ANN with 4 hidden layers.[85] The CT-FFR values based on machine learning and CFD were closely correlated (correlation coefficient $= 0.9994$, $P < 0.001$). Compared with invasive FFR, this method demonstrated high diagnostic proficiency: accuracy 83.2%, sensitivity 81.6%, specificity 83.9%, and correlation coefficient 0.729 ($P < 0.001$). Another important advantage is that FFR based on deep learning can be run offline using individual equipment, and the average calculation time is 196 s, shorter than that of CFD-based methods. The study by Tesche suggested that CT-FFR based on deep learning had a similar diagnostic value for regarding ischaemic pathologies to that of the computational fluid dynamics-based Siemens Healthineers model (AUC: 0.89 vs. 0.89).[86] The MACHINE study (Machine Learning Based CT Angiography Derived FFR: A Multi-Center Registry) showed an accuracy of 78% for FFR_{ML} in predicting stenosis with an FFR < 0.8, and the AUC was 0.84. In addition, in vessels with low to medium calcifications (Agatston > 0 to < 400), FFR_{ML} had a superior diagnostic value to that of visual evaluation through CCTA (AUC: 0.86 vs. 0.63, $P < 0.001$).[53]

Previous studies have suggested that deep learning contributes greatly to the early diagnosis and prognosis of lung cancer.[77] Convolutional neural networks (CNNs) also have good predictive value for coronary stenosis presenting as left ventricular ischaemia on CCTA. Two studies showed AUCs of 0.76 and 0.74.[87] Denzinger et al. discussed the use of several approaches combining radiomics and machine learning in plaque evaluation. The study performed dimensionality reduction on radiomics parameters using XGBoost.[88] Deep learning was combined with multiplanar reformat and CNNs. Gated recurrent units were used in the output layer. The risk model that combined radiomics and deep learning demonstrated the best predictive values for coronary stenosis with an AUC of 0.96 and accuracy of 92%. Regarding the evaluation of revascularization strategies, the above risk model also outperformed models based on radiomics and XGBoost or ANN alone. The results indicated that a more accurate evaluation of coronary plaques could be made by combining radiomics and deep learning.

Machine learning offers a new direction in the analysis of CCTA images and parameters. Advanced mathematical analysis contributes to the accurate fitting of risk models, and the image processing ability of ANNs has already exceeded human limits. Although the methodology of machine learning deviates from conventional statistical analysis and certain changes were made to the

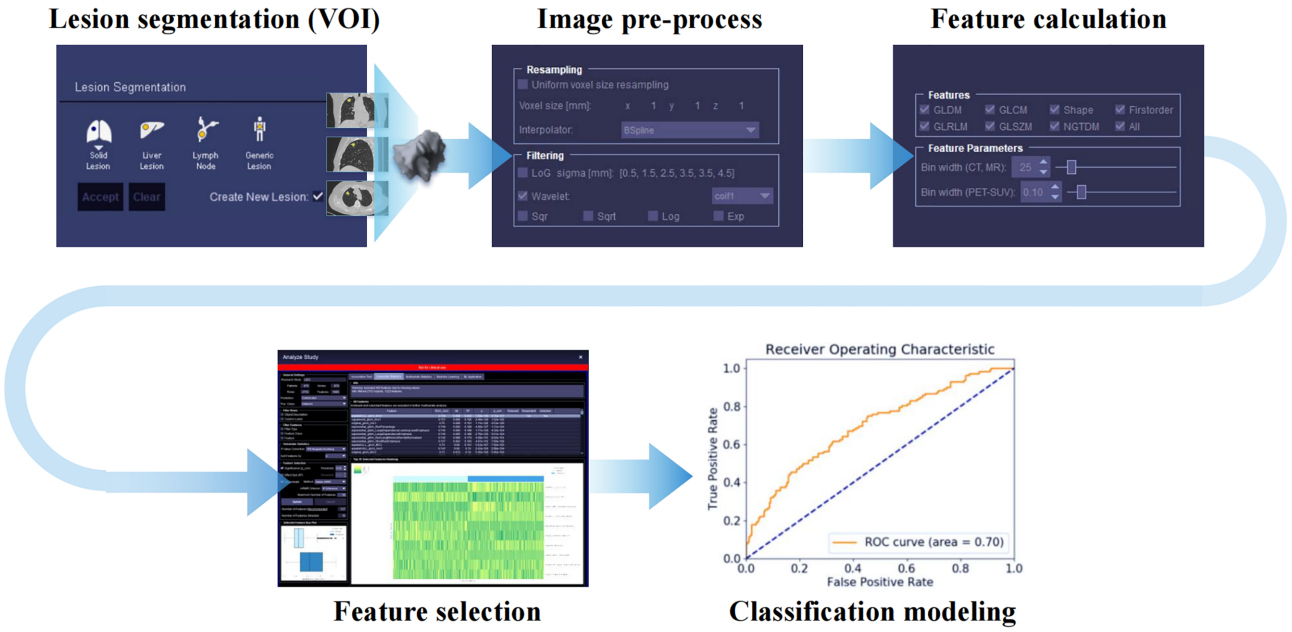

Figure 1. The process from lesion to risk model based on radiomic and machine learning by Siemens (Healthineers, Forchheim, Germany).

parameters (e.g. sensitivity in statistics was changed into recall rate in machine learning), the ability of machine learning to classify and predict outcomes of unknown data sets offers significant potential for the establishment of risk models in clinical management. To date, several clinical trials have built risk models in accordance with the TRIPOD guidelines based on machine learning.[89] Nonetheless, machine learning still faces many obstacles in data collection, training set volume, and interpretability. Solving those obstacles requires the joint efforts of physicians and data scientists.

Future perspectives

Apart from improvements to CT imaging technology, we should also focus on how to gain as much clinical information as possible from existing CCTA images. Applying physics models, new algorithms and image-processing technology provides a more detailed interpretation of CCTA images and enables physicians to conduct a more accurate and quantitative analysis. In addition to CCTA, deep learning has also achieved superiority over physician evaluations in the recognition of atherosclerotic plaques on OCT; however, the background noise or irrelevant pixels can decrease the accuracy of ANNs. This is a problem faced in CT imaging and many other clinical practices. Quantitative features of HRPs can be obtained through the observation and extraction of plaque features via radiomics. Currently, feature fitting conducted in machine learning enhances the proficiency of risk models. However, due to the unequal distribution of clinical data, small samples and inadequate application of study results, the development of AI in medicine is still in the preliminary stage. Moreover, novel algorithms such as reinforcement learning have already exhibited promising proficiency in clinical practice. The effective combination of these algorithms with radiology or clinical data on cardiovascular diseases still needs to be explored and awaits solutions from computer scientists and physicians. Regarding the technical challenges posed by radiomics and machine learning, in addition to multidisciplinary collaborations, online platforms are rapidly emerging. For instance, the platform founded by Siemens (Healthineers, Forchheim, Germany) provides a one-station extraction of radiomics features as well as the establishment of risk models based on PyRadiomics and random forest and is extremely beneficial in lowering the learning costs of radiology imaging analysis (Fig. 1).[90] As a noninvasive imaging modality, CCTA is more acceptable to patients as an alternative to ICA. Over the past two decades, it has been proven to be safe, effective, and feasible. Based on the provided three-dimensional information, CCTA is able to delineate and evaluate coronary arteries and its associated lesions in great detail.[91] CCTA-derived risk assessment tools are relatively simple for physicians to implement into daily clinical practice. For most patients, anatomical features such as degree of stenosis, calcification score, and HRP features demonstrated promising results in terms of predicting cardiovascular adverse events. As for patients with borderline stenosis (stenosis degree of 50%–75%), CT-FFR also plays a vital role in clinical decision making. Combined with machine learning and platforms of neural network, these tools are able to conduct a more comprehensive evaluation of CAD patients based on CCTA imaging as well as baseline characteristics. Under the emerging trend of multidisciplinary collaborations, CCTA holds great potential for providing a more accurate diagnosis and evaluation in multiple dimensions (Fig. 2).

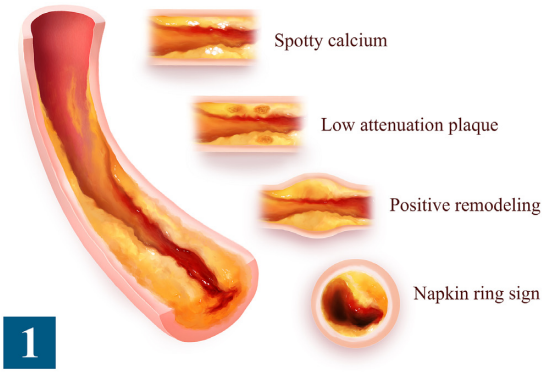

1 **Analysis the data from anatomical characteristics and morphological feature.**

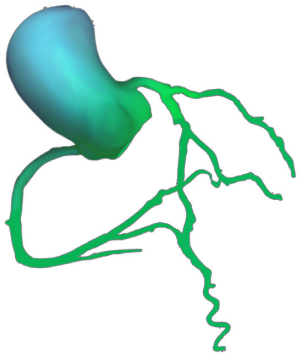

2 **Image post-processing to calculate the CT-FFR.**

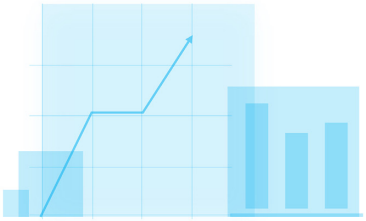

3 **Quantitative analysis of lesions features with radiomics.**

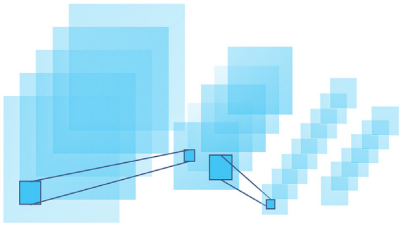

4 **Learning to learn with CCTA data or image.**

Figure 2. Using coronary computed tomographic angiography to perform risk assessment in patients with coronary disease in multiple dimensions.

Conclusions

The development of cardiac imaging is attributable to improvements in CT technology. Because of the emergence of CCTA, noninvasive evaluations of CAD and quick risk stratifications of patients have risen to a new level. The radiation exposure associated with CT examinations still presents a health concern for patients, especially when multiple examinations are required to obtain a consecutive picture of the disease. However, new methodologies and image-processing technologies have promoted comprehensive evaluations by CCTA based on multiple aspects, such as the degree of stenosis, plaque features, and functional reserve. Moreover, radiomics and machine learning provide an objective mathematical foundation and method for accurately evaluating of CCTA images. In the era of big data analytics and AI, CCTA will definitely be well-equipped to perform multidimensional risk stratifications of CAD patients.

Author contributions

Yiming Li: Conceptualization, Methodology, Writing—Original draft preparation. **Kaiyu Jia:** Investigation, Writing—Original draft preparation. **Yuheng Jia:** Writing—Original draft preparation, Writing—Reviewing and Editing. **Yong Yang:** Data curation, formal analysis. **Yijun Yao:** Visualization. **Mao Chen:** Supervision, funding acquisition. **Yong Peng:** funding acquisition, conceptualization.

Acknowledgements

This study was supported by the National Natural Science Foundation of China (Grant No. 81400267), Postdoctoral fellow support fund from Sichuan University (Grant No. 20826041E4070), and Sichuan Science and Technology Program (Grant No. 2021YFS0330).

Conflict of interest

Yiming Li, Kaiyu Jia, Yuheng Jia, Yong Yang, Yijun Yao, Mao Chen, and Yong Peng declare that they have no conflicts of interest. This article does not include any studies with human or animal subjects. This manuscript is a review article and does not involve a research protocol requiring approval by the relevant institutional review board or ethics committee.

References

1. Joseph P, Leong D, McKee M, *et al.* Reducing the global burden of cardiovascular disease, Part 1: the epidemiology and risk factors. *Circ Res* 2017;**121**:677–94. doi:10.1161/circresaha.117.308903.
2. Jones WB, Riley CP, Reeves TJ, *et al.* Natural history of coronary artery disease. *Bull N Y Acad Med* 1972;**48**:1109–25.

3. Knuuti J, Wijns W, Saraste A, *et al.* 2019 ESC Guidelines for the diagnosis and management of chronic coronary syndromes. *Eur Heart J* 2020;**41**:407–77. doi:10.1093/eurheartj/ehz425.
4. Campeau L. Percutaneous radial artery approach for coronary angiography. *Cathet Cardiovasc Diagn* 1989;**16**:3–7. doi:10.1002/ccd.1810160103.
5. Huang D, Swanson EA, Lin CP, *et al.* Optical coherence tomography. *Science* 1991;**254**:1178–81. doi:10.1126/science.1957169.
6. Nissen SE, Yock P. Intravascular ultrasound: novel pathophysiological insights and current clinical applications. *Circulation* 2001;**103**:604–16. doi:10.1161/01.cir.103.4.604.
7. Schmitt JM, Xiang SH, Yung KM. Speckle in optical coherence tomography. *J Biomed Opt* 1999;**4**:95–105. doi:10.1117/1.429925.
8. Abdulla J, Abildstrom SZ, Gotzsche O, *et al.* 64-multislice detector computed tomography coronary angiography as potential alternative to conventional coronary angiography: a systematic review and meta-analysis. *Eur Heart J* 2007;**28**:3042–50. doi:10.1093/eurheartj/ehm466.
9. Budoff MJ, Dowe D, Jollis JG, *et al.* Diagnostic performance of 64-multidetector row coronary computed tomographic angiography for evaluation of coronary artery stenosis in individuals without known coronary artery disease: results from the prospective multicenter ACCURACY (Assessment by Coronary Computed Tomographic Angiography of Individuals Undergoing Invasive Coronary Angiography) trial. *J Am Coll Cardiol* 2008;**52**:1724–32. doi:10.1016/j.jacc.2008.07.031.
10. Hoffmann U, Ferencik M, Cury RC, *et al.* Coronary CT angiography. *J Nucl Med* 2006;**47**:797–806.
11. Miller JM, Rochitte CE, Dewey M, *et al.* Diagnostic performance of coronary angiography by 64-row CT. *N Engl J Med* 2008;**359**:2324–36. doi:10.1056/NEJMoa0806576.
12. Cheezum MK, Blankstein R. Coronary computed tomographic angiography: its role in emergency department triage. *Circulation* 2014;**130**:2052–6. doi:10.1161/circulationaha.114.009648.
13. Hulten E, Pickett C, Bittencourt MS, *et al.* Outcomes after coronary computed tomography angiography in the emergency department: a systematic review and meta-analysis of randomized, controlled trials. *J Am Coll Cardiol* 2013;**61**:880–92. doi:10.1016/j.jacc.2012.11.061.
14. Hadamitzky M, Freissmuth B, Meyer T, *et al.* Prognostic value of coronary computed tomographic angiography for prediction of cardiac events in patients with suspected coronary artery disease. *JACC Cardiovasc Imaging* 2009;**2**:404–11. doi:10.1016/j.jcmg.2008.11.015.
15. Min JK, Shaw LJ, Devereux RB, *et al.* Prognostic value of multidetector coronary computed tomographic angiography for prediction of all-cause mortality. *J Am Coll Cardiol* 2007;**50**:1161–70. doi:10.1016/j.jacc.2007.03.067.
16. Chow BJ, Small G, Yam Y, *et al.* Incremental prognostic value of cardiac computed tomography in coronary artery disease using CONFIRM: COroNary computed tomography angiography evaluation for clinical outcomes: an InteRnational Multicenter registry. *Circ Cardiovasc Imaging* 2011;**4**:463–72. doi:10.1161/circimaging.111.964155.
17. Schulman-Marcus J, Lin FY, Gransar H, *et al.* Coronary revascularization vs. medical therapy following coronary-computed tomographic angiography in patients with low-, intermediate- and high-risk coronary artery disease: results from the CONFIRM long-term registry. *Eur Heart J Cardiovasc Imaging* 2017;**18**:841–8. doi:10.1093/ehjci/jew287.
18. Hadamitzky M, Achenbach S, Al-Mallah M, *et al.* Optimized prognostic score for coronary computed tomographic angiography: results from the CONFIRM registry (COronary CT Angiography EvaluatioN For Clinical Outcomes: An InteRnational Multicenter Registry). *J Am Coll Cardiol* 2013;**62**:468–76. doi:10.1016/j.jacc.2013.04.064.
19. Cury RC, Abbara S, Achenbach S, *et al.* Coronary Artery Disease—Reporting and Data System (CAD-RADS): An Expert Consensus Document of SCCT, ACR and NASCI: Endorsed by the ACC. *JACC Cardiovasc Imaging* 2016;**9**:1099–113. doi:10.1016/j.jcmg.2016.05.005.
20. Xie JX, Cury RC, Leipsic J, *et al.* The coronary artery disease-reporting and data system (CAD-RADS): Prognostic and clinical implications associated with standardized coronary computed tomography angiography reporting. *JACC Cardiovasc Imaging* 2018;**11**:78–89. doi:10.1016/j.jcmg.2017.08.026.
21. Cohen MC, Aretz TH. Histological analysis of coronary artery lesions in fatal postoperative myocardial infarction. *Cardiovasc Pathol* 1999;**8**:133–9. doi:10.1016/s1054-8807(98)00032-5.
22. Nasu K, Tsuchikane E, Katoh O, *et al.* Accuracy of in vivo coronary plaque morphology assessment: a validation study of in vivo virtual histology compared with in vitro histopathology. *J Am Coll Cardiol* 2006;**47**:2405–12. doi:10.1016/j.jacc.2006.02.044.
23. Gössl M, Versari D, Hildebrandt H, *et al.* Vulnerable plaque: detection and management. *Med Clin North Am* 2007;**91**:573–601; ix-x. doi:10.1016/j.mcna.2007.03.004.
24. Arbab-Zadeh A, Nakano M, Virmani R, *et al.* Acute coronary events. *Circulation* 2012;**125**:1147–56. doi:10.1161/circulationaha.111.047431.
25. Crea F, Libby P. Acute coronary syndromes: the way forward from mechanisms to precision treatment. *Circulation* 2017;**136**:1155–66. doi:10.1161/circulationaha.117.029870.
26. Finn AV, Nakano M, Narula J, *et al.* Concept of vulnerable/unstable plaque. *Arterioscler Thromb Vasc Biol* 2010;**30**:1282–92. doi:10.1161/atvbaha.108.179739.
27. Virmani R, Burke AP, Farb A, *et al.* Pathology of the vulnerable plaque. *J Am Coll Cardiol* 2006;**47**:C13–8. doi:10.1016/j.jacc.2005.10.065.
28. Davies MJ. Acute coronary thrombosis—the role of plaque disruption and its initiation and prevention. *Eur Heart J* 1995;**16**:3–7. doi:10.1093/eurheartj/16.suppl_l.3.
29. Mann JM, Davies MJ. Vulnerable plaque. Relation of characteristics to degree of stenosis in human coronary arteries. *Circulation* 1996;**94**:928–31. doi:10.1161/01.cir.94.5.928.
30. Pflederer T, Marwan M, Schepis T, *et al.* Characterization of culprit lesions in acute coronary syndromes using coronary dual-source CT angiography. *Atherosclerosis* 2010;**211**:437–44. doi:10.1016/j.atherosclerosis.2010.02.001.
31. Puchner SB, Liu T, Mayrhofer T, *et al.* High-risk plaque detected on coronary CT angiography predicts acute coronary syndromes independent of significant stenosis in acute chest pain: results from the ROMICAT-II trial. *J Am Coll Cardiol* 2014;**64**:684–92. doi:10.1016/j.jacc.2014.05.039.
32. Leber AW, Knez A, White CW, *et al.* Composition of coronary atherosclerotic plaques in patients with acute myocardial infarction and stable angina pectoris determined by contrast-enhanced multislice computed tomography. *Am J Cardiol* 2003;**91**:714–8. doi:10.1016/s0002-9149(02)03411-2.
33. Motoyama S, Ito H, Sarai M, *et al.* Plaque characterization by coronary computed tomography angiography and the likelihood of acute coronary events in mid-term follow-up. *J Am Coll Cardiol* 2015;**66**:337–46. doi:10.1016/j.jacc.2015.05.069.

34. van Velzen JE, de Graaf FR, de Graaf MA, *et al*. Comprehensive assessment of spotty calcifications on computed tomography angiography: comparison to plaque characteristics on intravascular ultrasound with radiofrequency backscatter analysis. *J Nucl Cardiol* 2011;**18**:893–903. doi:10.1007/s12350-011-9428-2.
35. Maurovich-Horvat P, Hoffmann U, Vorpahl M, *et al*. The napkin-ring sign: CT signature of high-risk coronary plaques? *JACC Cardiovasc Imaging* 2010;**3**:440–4. doi:10.1016/j.jcmg.2010.02.003.
36. Thomsen C, Abdulla J. Characteristics of high-risk coronary plaques identified by computed tomographic angiography and associated prognosis: a systematic review and meta-analysis. *Eur Heart J Cardiovasc Imaging* 2016;**17**:120–9. doi:10.1093/ehjci/jev325.
37. Nerlekar N, Ha FJ, Cheshire C, *et al*. Computed tomographic coronary angiography-derived plaque characteristics predict major adverse cardiovascular events: a systematic review and meta-analysis. *Circ Cardiovasc Imaging* 2018;**11**:e006973. doi:10.1161/circimaging.117.006973.
38. Ferencik M, Mayrhofer T, Puchner SB, *et al*. Computed tomography-based high-risk coronary plaque score to predict acute coronary syndrome among patients with acute chest pain—results from the ROMICAT II trial. *J Cardiovasc Comput Tomogr* 2015;**9**:538–45. doi:10.1016/j.jcct.2015.07.003.
39. Yang Y, Shah JP, Zeng H, *et al*. Prevalence and prognosis of high-risk plaque on coronary CT angiography in hospitalized patients. *JACC Cardiovasc Imaging* 2020;**13**:522–3. doi:10.1016/j.jcmg.2019.08.016.
40. Antonopoulos AS, Sanna F, Sabharwal N, *et al*. Detecting human coronary inflammation by imaging perivascular fat. *Sci Transl Med* 2017;**9**(398):eaal2658. doi:10.1126/scitranslmed.aal2658.
41. Oikonomou EK, Marwan M, Desai MY, *et al*. Non-invasive detection of coronary inflammation using computed tomography and prediction of residual cardiovascular risk (the CRISP CT study): a post-hoc analysis of prospective outcome data. *Lancet* 2018;**392**:929–39. doi:10.1016/s0140-6736(18)31114-0.
42. Pijls NH, De Bruyne B, Peels K, *et al*. Measurement of fractional flow reserve to assess the functional severity of coronary-artery stenoses. *N Engl J Med* 1996;**334**:1703–8. doi:10.1056/nejm199606273342604.
43. De Bruyne B, Pijls NH, Kalesan B, *et al*. Fractional flow reserve-guided PCI versus medical therapy in stable coronary disease. *N Engl J Med* 2012;**367**:991–1001. doi:10.1056/NEJMoa1205361.
44. Pellicano M, De Bruyne B, Toth GG, *et al*. Fractional flow reserve to guide and to assess coronary artery bypass grafting. *Eur Heart J* 2017;**38**:1959–68. doi:10.1093/eurheartj/ehw505.
45. Tonino PA, De Bruyne B, Pijls NH, *et al*. Fractional flow reserve versus angiography for guiding percutaneous coronary intervention. *N Engl J Med* 2009;**360**:213–24. doi:10.1056/NEJMoa0807611.
46. Kolh P, Windecker S. ESC/EACTS myocardial revascularization guidelines 2014. *Eur Heart J* 2014;**35**:3235–6. doi:10.1093/eurheartj/ehu422.
47. Zarins CK, Taylor CA, Min JK. Computed fractional flow reserve (FFTCT) derived from coronary CT angiography. *J Cardiovasc Transl Res* 2013;**6**:708–14. doi:10.1007/s12265-013-9498-4.
48. Taylor CA, Fonte TA, Min JK. Computational fluid dynamics applied to cardiac computed tomography for noninvasive quantification of fractional flow reserve: scientific basis. *J Am Coll Cardiol* 2013;**61**:2233–41. doi:10.1016/j.jacc.2012.11.083.
49. Koo BK, Erglis A, Doh JH, *et al*. Diagnosis of ischemia-causing coronary stenoses by noninvasive fractional flow reserve computed from coronary computed tomographic angiograms. Results from the prospective multicenter DISCOVER-FLOW (Diagnosis of Ischemia-Causing Stenoses Obtained Via Noninvasive Fractional Flow Reserve) study. *J Am Coll Cardiol* 2011;**58**:1989–97. doi:10.1016/j.jacc.2011.06.066.
50. Min JK, Leipsic J, Pencina MJ, *et al*. Diagnostic accuracy of fractional flow reserve from anatomic CT angiography. *JAMA* 2012;**308**:1237–45. doi:10.1001/2012.jama.11274.
51. Nørgaard BL, Leipsic J, Gaur S, *et al*. Diagnostic performance of noninvasive fractional flow reserve derived from coronary computed tomography angiography in suspected coronary artery disease: the NXT trial (Analysis of Coronary Blood Flow Using CT Angiography: Next Steps). *J Am Coll Cardiol* 2014;**63**:1145–55. doi:10.1016/j.jacc.2013.11.043.
52. Baumann S, Renker M, Hetjens S, *et al*. Comparison of coronary computed tomography angiography-derived vs invasive fractional flow reserve assessment: meta-analysis with subgroup evaluation of intermediate stenosis. *Acad Radiol* 2016;**23**:1402–11. doi:10.1016/j.acra.2016.07.007.
53. Coenen A, Kim YH, Kruk M, *et al*. Diagnostic accuracy of a machine-learning approach to coronary computed tomographic angiography-based fractional flow reserve: Result from the MACHINE consortium. *Circ Cardiovasc Imaging* 2018;**11**:e007217. doi:10.1161/circimaging.117.007217.
54. Renker M, Schoepf UJ, Wang R, *et al*. Comparison of diagnostic value of a novel noninvasive coronary computed tomography angiography method versus standard coronary angiography for assessing fractional flow reserve. *Am J Cardiol* 2014;**114**:1303–8. doi:10.1016/j.amjcard.2014.07.064.
55. Wang ZQ, Zhou YJ, Zhao YX, *et al*. Diagnostic accuracy of a deep learning approach to calculate FFR from coronary CT angiography. *J Geriatr Cardiol* 2019;**16**:42–8. doi:10.11909/j.issn.1671-5411.2019.01.010.
56. Benton SM, Jr., Tesche C, De Cecco CN, *et al*. Noninvasive derivation of fractional flow reserve from coronary computed tomographic angiography: a review. *J Thorac Imaging* 2018;**33**:88–96. doi:10.1097/rti.0000000000000289.
57. Hlatky MA, De Bruyne B, Pontone G, *et al*. Quality-of-life and economic outcomes of assessing fractional flow reserve with computed tomography angiography: PLATFORM. *J Am Coll Cardiol* 2015;**66**:2315–23. doi:10.1016/j.jacc.2015.09.051.
58. Fairbairn TA, Nieman K, Akasaka T, *et al*. Real-world clinical utility and impact on clinical decision-making of coronary computed tomography angiography-derived fractional flow reserve: lessons from the ADVANCE Registry. *Eur Heart J* 2018;**39**:3701–11. doi:10.1093/eurheartj/ehy530.
59. Lee JM, Choi G, Koo BK, *et al*. Identification of high-risk plaques destined to cause acute coronary syndrome using coronary computed tomographic angiography and computational fluid dynamics. *JACC Cardiovasc Imaging* 2019;**12**:1032–43. doi:10.1016/j.jcmg.2018.01.023.
60. Park J, Lee JM, Koo BK, *et al*. Relevance of anatomical, plaque, and hemodynamic characteristics of non-obstructive coronary lesions in the prediction of risk for acute coronary syndrome. *Eur Radiol* 2019;**29**:6119–28. doi:10.1007/s00330-019-06221-9.
61. Lambin P, Rios-Velazquez E, Leijenaar R, *et al*. Radiomics: extracting more information from medical images using advanced feature analysis. *Eur J Cancer* 2012;**48**:441–6. doi:10.1016/j.ejca.2011.11.036.

62. Hell MM, Motwani M, Otaki Y, *et al*. Quantitative global plaque characteristics from coronary computed tomography angiography for the prediction of future cardiac mortality during long-term follow-up. *Eur Heart J Cardiovasc Imaging* 2017;**18**:1331–9. doi:10.1093/ehjci/jex183.
63. Kolossváry M, Kellermayer M, Merkely B, *et al*. Cardiac computed tomography radiomics: a comprehensive review on radiomic techniques. *J Thorac Imaging* 2018;**33**:26–34. doi:10.1097/rti.0000000000000268.
64. Haralick RM, Shanmugam K, Dinstein I. Textural features for image classification. *IEEE Trans Syst Man Cybern* 1973;**SMC-3**:610–21. doi:10.1109/TSMC.1973.4309314.
65. Galloway MM. Texture analysis using grey level run lengths. *Journal* 1974;**75**:18555.
66. Xinli W, Albregtsen F, Foyn B. Texture analysis using gray level gap length matrix. *Theory and Applications of Image Analysis* 1995;**II**: 65–78. doi:10.1142/9789812830579_0006.
67. Larkin TJ, Canuto HC, Kettunen MI, *et al*. Analysis of image heterogeneity using 2D Minkowski functionals detects tumor responses to treatment. *Magn Reson Med* 2014;**71**:402–10. doi:10.1002/mrm.24644.
68. Liu Z, Liu S. Random fractional Fourier transform. *Opt Lett* 2007;**32**:2088–90. doi:10.1364/ol.32.002088.
69. Kolossváry M, Karády J, Szilveszter B, *et al*. Radiomic features are superior to conventional quantitative computed tomographic metrics to identify coronary plaques with napkin-ring sign. *Circ Cardiovasc Imaging* 2017;**10**:e006843. doi:10.1161/circimaging.117.006843.
70. Kolossváry M, Karády J, Kikuchi Y, *et al*. Radiomics versus visual and histogram-based assessment to identify atheromatous lesions at coronary CT angiography: an ex vivo study. *Radiology* 2019;**293**:89–96. doi:10.1148/radiol.2019190407.
71. Nam K, Suh YJ, Han K, *et al*. Value of computed tomography radiomic features for differentiation of periprosthetic mass in patients with suspected prosthetic valve obstruction. *Circ Cardiovasc Imaging* 2019;**12**:e009496. doi:10.1161/circimaging.119.009496.
72. Dimitrakopoulos GN, Vrahatis AG, Plagianakos V, *et al*. Pathway analysis using XGBoost classification in Biomedical Data. *Proceedings of the 10th Hellenic Conference on Artificial Intelligence* 2018;Artcile 16;1–6. doi: 10.1145/3200947.3201029.
73. Rajkomar A, Dean J, Kohane I. Machine learning in medicine. *N Engl J Med* 2019;**380**:1347–58. doi:10.1056/NEJMra1814259.
74. Ching T, Himmelstein DS, Beaulieu-Jones BK, *et al*. Opportunities and obstacles for deep learning in biology and medicine. *J R Soc Interface* 2018;**15**(141). doi:10.1098/rsif.2017.0387.
75. Lee JG, Jun S, Cho YW, *et al*. Deep learning in medical imaging: general overview. *Korean J Radiol* 2017;**18**:570–84. doi:10.3348/kjr.2017.18.4.570.
76. Chen L, Xia C, Sun H. Recent advances of deep learning in psychiatric disorders. *Precision Clinical Medicine* 2020;**3**:202–13. doi:10.1093/pcmedi/pbaa029.
77. Zhou Y, Xu X, Song L, *et al*. The application of artificial intelligence and radiomics in lung cancer. *Precision Clinical Medicine* 2020;**3**:214–27. doi:10.1093/pcmedi/pbaa028.
78. Mittal S, Zheng Y, Georgescu B, *et al*. Fast automatic detection of calcified coronary lesions in 3D cardiac CT images. *Machine Learning in Medical Imaging* 2010, pp.1–9. doi: 10.1007/978-3-642-15948-0_1.
79. Yang G, Chen Y, Ning X, *et al*. Automatic coronary calcium scoring using noncontrast and contrast CT images. *Med Phys* 2016;**43**:2174. doi:10.1118/1.4945045.
80. Dey D, Gaur S, Ovrehus KA, *et al*. Integrated prediction of lesion-specific ischaemia from quantitative coronary CT angiography using machine learning: a multicentre study. *Eur Radiol* 2018;**28**:2655–64. doi:10.1007/s00330-017-5223-z.
81. Kang D, Dey D, Slomka PJ, *et al*. Structured learning algorithm for detection of nonobstructive and obstructive coronary plaque lesions from computed tomography angiography. *J Med Imaging (Bellingham)* 2015;**2**:014003. doi:10.1117/1.Jmi.2.1.014003.
82. Kwan AC, McElhinney PA, Tamarappoo BK, *et al*. Prediction of revascularization by coronary CT angiography using a machine learning ischemia risk score. *Eur Radiol* 2021;**31**:1227–35. doi:10.1007/s00330-020-07142-8.
83. Motwani M, Dey D, Berman DS, *et al*. Machine learning for prediction of all-cause mortality in patients with suspected coronary artery disease: a 5-year multicentre prospective registry analysis. *Eur Heart J* 2017;**38**:500–7. doi:10.1093/eurheartj/ehw188.
84. van Rosendael AR, Maliakal G, Kolli KK, *et al*. Maximization of the usage of coronary CTA derived plaque information using a machine learning based algorithm to improve risk stratification; insights from the CONFIRM registry. *J Cardiovasc Comput Tomogr* 2018;**12**:204–9. doi:10.1016/j.jcct.2018.04.011.
85. Itu L, Rapaka S, Passerini T, *et al*. A machine-learning approach for computation of fractional flow reserve from coronary computed tomography. *J Appl Physiol (1985)* 2016;**121**:42–52. doi:10.1152/japplphysiol.00752.2015.
86. Tesche C, De Cecco CN, Baumann S, *et al*. Coronary CT angiography-derived fractional flow reserve: machine learning algorithm versus computational fluid dynamics modeling. *Radiology* 2018;**288**:64–72. doi:10.1148/radiol.2018171291.
87. van Hamersvelt RW, Zreik M, Voskuil M, *et al*. Deep learning analysis of left ventricular myocardium in CT angiographic intermediate-degree coronary stenosis improves the diagnostic accuracy for identification of functionally significant stenosis. *Eur Radiol* 2019;**29**:2350–9. doi:10.1007/s00330-018-5822-3.
88. Denzinger F, Wels M, Ravikumar N, *et al*. *Medical Image Computing and Computer-Assisted Intervention* 2019; 593–601.
89. Collins GS, Moons KGM. Reporting of artificial intelligence prediction models. *Lancet* 2019;**393**:1577–9. doi:10.1016/s0140-6736(19)30037-6.
90. Wels M, Lades F, Muehlberg A, *et al*. General purpose radiomics for multi-modal clinical research.Proceedings of the SPIE, 2019. doi:10.1117/12.2511856.
91. Andrew M, John H. The challenge of coronary calcium on coronary computed tomographic angiography (CCTA) scans: effect on interpretation and possible solutions. *Int J Cardiovasc Imaging* 2015;**31**:145–57. doi:10.1007/s10554-015-0773-0.